

Forecasting climate change impacts on plant populations over large spatial extents

ANDREW T. TREDENNICK^{*1}, MEVIN B. HOOTEN^{2,3,4}, CAMERON L. ALDRIDGE⁵, COLLIN G. HOMER⁶, ANDREW R. KLEINHESSELINK¹, AND PETER B. ADLER¹

¹*Department of Wildland Resources and the Ecology Center, 5230 Old Main Hill, Utah State University, Logan, Utah 84322 USA*

²*U.S. Geological Survey, Colorado Cooperative Fish and Wildlife Research Unit, Colorado State University, Fort Collins, CO 80523 USA*

³*Department of Fish, Wildlife, and Conservation Biology, Colorado State University, Fort Collins, CO 80523 USA*

⁴*Department of Statistics, Colorado State University, Fort Collins, CO 80523 USA*

⁵*Natural Resource Ecology Laboratory and Department of Ecosystem Science and Sustainability, Colorado State University, Fort Collins, CO, in cooperation with US Geological Survey, Fort Collins Science Center, Fort Collins, CO*

⁶*U.S. Geological Survey (USGS) Earth Resources Observation and Science (EROS) Center, Sioux Falls, SD 57198 USA*

Abstract

Plant population models are powerful tools for predicting climate change impacts in one location, but are difficult to apply at landscape scales. We overcome this limitation by taking advantage of two recent advances: remotely-sensed, species-specific estimates of plant cover and statistical models developed for spatio-temporal dynamics of animal populations. Using computationally efficient model reparameterizations, we fit a spatiotemporal population model to a 28 year time series of sagebrush (*Artemisia* spp.) percent cover over

^{*}Corresponding author: atredenn@gmail.com

a 2.5×5 km landscape in southwestern Wyoming while formally accounting for spatial autocorrelation. We include interannual variation in precipitation and temperature as covariates in the model to investigate how climate affects the cover of sagebrush. We then use the model to forecast the future abundance of sagebrush at the landscape scale under projected climate change, generating spatially explicit estimates of change in a plant population that have, until now, been impossible to produce at this scale. Our broad-scale and long-term predictions are rooted in small-scale and short-term population dynamics and provide an alternative to predictions offered by species distribution models that do not include population dynamics. Our approach, which brings together several common techniques, is among the first steps toward using remote sensing data to model population responses to environmental change that play out at spatial scales far greater than the traditional field study plot.

Key words: population model, climate change, forecasting, spatiotemporal model, remote sensing, sagebrush, Artemisia, dimension reduction

Introduction

Forecasting the impacts of climate change on plant populations and communities is a central challenge for ecology (Clark et al. 2001, Petchey et al. 2015). Population models are ideally suited for meeting such a challenge because they provide a way to link climate drivers directly to population dynamics (Hare et al. 2010, Adler et al. 2012, Ross et al. 2015, Shriver 2015). However, inference from population models is typically limited to small spatial extents because the data required is difficult to collect across broad species ranges. Almost every study of plant population dynamics relies on demographic observations recorded at the meter to sub-meter scale (see, e.g., Salguero-Gómez et al. 2015). Local-scale demographic data make building population projection models an easy task (Ellner and Rees 2006, Rees and Ellner 2009, Adler et al. 2012), but it is very difficult

to extrapolate small-scale studies to large spatial extents with any certainty because the data likely only represent a small subset of parameter space and environmental conditions (Freckleton et al. 2011, Queenborough et al. 2011). The real challenge is not to simply make population forecasts, but to do so at spatial scales relevant to policy and management decisions (Queenborough et al. 2011).

The ideal tool would be a large-scale, dynamic population model (Schurr et al. 2012, Merow et al. 2014), but developing useful models at this scale has been limited by the availability of time series data at large spatial extents and statistical methods for fitting high-dimensional spatial models. Fortunately, new advances in remote sensing and statistics now allow us to overcome both of these limitations. First, new remote-sensing (RS) methods are now producing accurate time series of species-specific plant cover at landscape scales. These data can be fit with dynamic population models which include yearly fluctuations in climate as covariates. Such RS time series have revolutionized models of how climate affects ecosystem-level processes (e.g., Running et al. 2004) and have been used to detect long-term trends in plant population abundance (e.g., Homer et al. 2015), but they have yet to be used to drive a dynamic population model. Second, animal population modelers have developed dimension reduction and reparameterization techniques to efficiently fit high-dimension spatiotemporal models (see Conn et al. 2015 for a review). These new statistical methods have yet to be applied to RS-derived plant population data at broad scales.

Large-scale, spatially-explicit population models based on RS data could offer a valuable new way to investigate the effects of large-scale environmental changes playing out at landscape and regional scales. Most current assessments of how plant and animal populations will respond to climate change rely on species distribution models (SDMs). SDMs rely on static associations between contemporary climate and a species' distribution or, more rarely, abundance to project future distribution or abundance (Elith and Leathwick 2009) and they are easily applied at landscape to continental scales (e.g., Maiorano et al. 2013,

76 Clark et al. 2014). However, the short-term and small-scale population dynamics that
77 actually drive the large-scale distributions of species are not represented in most SDMs.
78 Because SDMs typically rely on occurrence data, their projections of habitat suitability or
79 probability of occurrence provide little information on the future states of populations in
80 the core of their range – areas where a species exists now and is expected to persist in the
81 future (Ehrlén and Morris 2015). Furthermore, because they lack short-term dynamics,
82 SDMs usually cannot produce any estimate of the rate at which local populations will
83 increase or decrease in the near-term and instead project a future equilibrium species dis-
84 tribution that may or may not ever be reached. Direct validation of such predictions is
85 extremely rare (Roberts and Hamann 2012). Large-scale dynamic population models could
86 overcome these limitations. They would produce spatially-explicit estimates of species
87 abundance within the species range (Ehrlén and Morris 2015), have the potential to model
88 expansion in abundance outside the range when coupled with dynamic models of dispersal,
89 and would provide testable predictions of how populations should respond to short-term
90 climate perturbations. These short-term predictions also would give modelers the opportu-
91 nity to repeatedly validate and refine their models (Luo et al. 2011).

92 Sagebrush (*Artemisia* spp.) ecosystems offer an ideal testing ground for new spatially ex-
93 plicit population models derived from RS data. Sagebrush species are widely distributed
94 (Kuchler 1964), they are sensitive to climate (Perfors et al. 2003, Miglia et al. 2005, Poore
95 et al. 2009, Dalglish et al. 2011, Xian et al. 2012, Apodaca 2013, Schlaepfer et al. 2014a,
96 2014b, Harte et al. 2015, Homer et al. 2015), new landscape and regional scale time series
97 of sagebrush cover are now being produced from aerial imagery (Homer et al. 2012), and
98 forecasts of future sagebrush ecosystems are in high demand due to the precarious conser-
99 vation status of the greater sage-grouse (*Centrocercus urophasianus*) (Arnett and Riley
100 2015). SDMs typically predict that much of the area occupied by sagebrush ecosystems
101 today will become unsuitable for sagebrush due to climate change, resulting in a dramatic
102 loss in the extent of sagebrush habitat by the end of this century (Shafer et al. 2001, Neil-

son et al. 2005, Bradley 2010, Schlaepfer et al. 2012, Still and Richardson 2015). Ecology models supply a possible mechanism for sagebrush losses predicted by SDMs: climate warming could lead to earlier snowmelt, increased evaporation and ultimately less recharge of deeper soil layers in the spring (Schlaepfer et al. 2012, Schlaepfer et al. 2014a). In warmer parts of its range, increased temperature could be especially detrimental to sagebrush as it depends on water from deeper soil to survive and grow in this arid region (Pechanec et al. 1937, Schlaepfer et al. 2011, Germino and Reinhardt 2014). In contrast, at higher elevations and in colder regions, warming and earlier snowmelt could lengthen the growing season and increase sagebrush occurrence (Schlaepfer et al. 2012, Schlaepfer et al. 2014a). Direct observations of individual plants and experimental plots tend to agree with these models: growth tends to respond negatively to spring and summer temperatures (Miglia et al. 2005, Poore et al. 2009, Apodaca 2013) except at higher elevations where earlier snowmelt may allow for a longer growing season (Perfors et al. 2003, Harte et al. 2015). A large-scale, spatially-explicit population model for sagebrush driven by interannual climate variability would provide a valuable new tool for assessing how sagebrush could respond to climate change in the future.

Building on recent technological advances in spatial statistics (Latimer et al. 2009, Conn et al. 2015) and anticipating ever-increasing availability of RS data (He et al. 2015), we demonstrate how large-scale plant population models could be used to predict population impacts of climate change. As a proof-of-concept, we use a process model motivated by Gompertz density-dependent population growth and a remotely-sensed time series of sagebrush cover from Wyoming (Homer et al. 2012, 2015). We account for spatial autocorrelation with dimension reduction techniques (Latimer et al. 2009, Conn et al. 2015) and produce spatially-explicit estimates of sagebrush percent cover. The modeling framework we propose can be applied to any spatially-explicit time series of plant cover or density, but its application to remotely-sensed data products offers the greatest potential to combine the information of population models (e.g., population status and temporal dynamics) and the

spatial extent of species distribution models.

Materials and Methods

Data

Remotely-sensed time series To demonstrate our modeling approach, we use a subset of a remotely-sensed time series of sagebrush (*Artemisia* spp.) canopy cover in Wyoming (Homer et al. 2012). As part of a separate study, Homer et al. 2012 estimated sagebrush percent cover using a regression tree to relate ground reflectances retrieved by three sources of optical imagery (QuickBird, Landsat, and AWiFS) to 1,780 field observations of sagebrush cover distributed across Wyoming. The regression tree model was further validated using another 297 field observations. For Wyoming sagebrush, the model achieved an $R^2 = 0.65$ and an out-of-sample RMSE of 5.46% (Homer et al. 2012). To hind-cast sagebrush cover the regression tree model was applied to historical remote sensing images to generate yearly predictions of sagebrush cover for all of Wyoming for the years 1984-2011. This resulted in an annual time series of sagebrush cover at 30 meter resolution from 1984 to 2011 (Fig. A1). In this remote sensing product, values represent the percentage of a 30×30 meter pixel covered by sagebrush. In our study, we focused on a $5,070 \times 2,430$ meter subset totaling 13,689 30×30 meter pixels each year (Fig. 1). Thus, the full remote sensing product contains 369,603 observations spanning 27 year-to-year transitions (27 years \times 13,689 pixels).

Climate covariates Our approach models interannual changes in plant cover as a function of seasonal climate variables. We used daily historic weather data for the center of our study site from the NASA Daymet data set (*available online*)¹. The Daymet weather data are interpolated between coarse observation units and capture some spatial variation.

¹<http://daymet.ornl.gov/>

We relied on weather data for the centroid of our study area. We calculated five climate variables from the Daymet data for the time period coinciding with our remotely sensed data (1984 to 2011).

We narrowed our focus to climate covariates we know are important for sagebrush and that could be calculated from general circulation model projections. The five climate variables in our population model are: (1) cumulative, “water year” precipitation for year $t-2$ ($lagPpt$), (2) year $t-1$ fall through summer precipitation ($ppt1$), (3) year t fall through summer precipitation ($ppt2$), (4) year $t-1$ average spring temperature ($TmeanSpr1$), and (5) year t average spring temperature ($TmeanSpr2$), where $t-1$ to t is the transition of interest. We selected these variables *a priori* based on previous studies (see *Introduction*), though not all emerge as important predictors in our model.

Additive spatio-temporal model for sagebrush cover

We use a descriptive model for sagebrush cover that includes additive spatial and temporal effects similar to that described by Conn et al. (2015). Interannual change in percent cover represents the integrated outcome of recruitment, survival, growth, and retrogression (shrinkage) of individual plants from year to year. We model observed integer percent cover (y) in cell i at time t as conditionally Poisson

$$y_{i,t} \sim \text{Poisson}(\mu_{i,t}), \quad (1)$$

where $\mu_{i,t}$ is the expected percent cover of pixel i in year t

$$\log(\mu_{i,t}) = \underbrace{\beta_{0,t} + \beta_1 y_{i,t-1}}_{\text{temporal} + \text{dens. dep}} + \underbrace{\mathbf{x}_t' \boldsymbol{\gamma}}_{\text{climate}} + \underbrace{\eta_i}_{\text{spatial}}. \quad (2)$$

Our model of percent cover change includes a density-dependent effect of log-transformed cover in the previous year ($y_{i,t-1}$), climate effects (\mathbf{x}_t), and a spatial random effect (η) for each pixel i . Climate effects were standardized $[(x_i - \bar{x})/\sigma(x)]$ to improve convergence during the model fitting stage and to allow for easier prior specification. The intercept, $\beta_{0,t}$, was allowed to vary through time; these random year effects recognize that all observations

from a particular year share the same climate covariates and thus are not independent. We used a Poisson likelihood because integer percent cover values in the sagebrush data product can be considered a form of count data. We also evaluated a negative binomial model, but found little evidence for overdispersion beyond what our model was already accomodating via the spatial random effects (η). There was no evidence of zero-inflation in our data, but see below (*Accomodating zeros*) for how we handled the small number of zero percent cover observations. We assume that the remotely sensed estimates of percent cover are "true" and free of error. This need not be the case, and if measurement error is known then it could be included in our Bayesian model as a "data model" (Hobbs and Hooten 2015).

The spatial random effect (η) accounts for spatial autocorrelation among pixels that occur near each other in space. Thus, η acts as an offset on the intercept ($\beta_{0,t}$), creating a spatial field that defines how pixels differ from the mean, on average, in space (e.g., areas of perennially low or high cover, relative to average cover). Fitting the model with a spatial random effect (η) is computationally demanding for large data sets like ours. The computational demand is due to the required calculations of the spatial covariance matrices, which increase as a cubic function of the number of locations (Wikle 2010). Key to our approach is a dimension reduction strategy that greatly reduces the number of parameters needed to be estimated to account for spatial variation by reducing the size of the spatial covariance matrices that need to be inverted at each MCMC iteration. Fitting models that appropriately account for spatial autocorrelation over large spatial extents would not be feasible without these modern techniques. Our dimension reduction strategy expresses the high dimensional spatial random effect, η , as the product of an expansion matrix, \mathbf{K} , and a smaller parameter vector, α (e.g., Hooten et al. 2003, Hooten and Wikle 2007, Conn et al. 2015). We can then approximate the spatial effect as

$$\boldsymbol{\eta} \approx \mathbf{K}\boldsymbol{\alpha}, \quad (3)$$

$$\alpha_m \sim \text{Normal}(0, \sigma_\eta^2). \quad (4)$$

204 In this case, $\boldsymbol{\alpha}$ is a $m \times 1$ vector of reduced spatial random effects, and \mathbf{K} is a $S \times m$ matrix
 205 that maps the reduced effects to the full S -dimensional space, where S is the total number
 206 of observed locations. Thus, we are able to reduce the effective number of parameters from
 207 S to m .

208 The last remaining obstacle is to parameterize the matrix of basis functions, \mathbf{K} . We use
 209 kernel convolution (Barry and Hoef 1996, Higdon 1998) to interpolate the spatial random
 210 effect between m “knots” that are nonrandomly distributed across the space of our study
 211 area. This means we are modeling spatial random effects at the knot level, and we use \mathbf{K}
 212 to interpolate those effects between knots. We use an exponential kernel density to define
 213 the distance-decay function around the knots (\mathbf{w}), such that the entries of \mathbf{K} are

$$K_{s,m} = w_{s,m} / \sum_{s=1}^S w_{s,m} \quad (5)$$

215 where

$$w_{s,m} = \exp\left(\frac{-d_{s,m}}{\sigma}\right) \quad (6)$$

217 and $d_{s,m}$ is the Euclidean distance between the centroid of sample cell s and the location
 218 of knot m , and σ is the kernel bandwidth. It is possible, through exhaustive model se-
 219 lection and fitting, to determine the optimal form of the kernel and to estimate optimal
 220 values for σ (Higdon 2002, Hooten and Hobbs 2015). However, given the relative size of
 221 our dataset and computational limitations, we defined kernels around 231 knots (Fig. B2)
 222 whose nearest neighbor distances are approximately equal to the range of spatial depen-
 223 dence in residuals from a simple GLM fit without climate covariates and the spatial ran-
 224 dom effect (~ 500 meters; Appendix B). An infinite number of knots would result in an
 225 exact representation of the spatial process and covariance model. Computationally, using
 226 an infinite number of knots is not possible, thus the use of dimension reduction techniques

227 serves as an approximation, where the accuracy increases with the number of knots. Given
 228 the tradeoff between knot number and computation time, we chose to base our knot num-
 229 ber on the spatial dependence as described above.

230 The Bayesian posterior distribution of our spatio-temporal model can be expressed as

$$[\boldsymbol{\beta}, \boldsymbol{\gamma}, \boldsymbol{\alpha}, \sigma_\eta^2 | \mathbf{y}] \propto \left(\prod_{t=1}^T \prod_{i=1}^n [y_{i,t} | \beta_{0,t}, \beta_1, \boldsymbol{\gamma}, \boldsymbol{\alpha}] [\beta_{0,t} | \bar{\beta}_0, \sigma_{\bar{\beta}_0}^2] \right) \times \quad (7)$$

$$\left(\prod_{m=1}^M [\alpha_m | \sigma_\eta^2] \right) [\bar{\beta}_0] [\beta_1] [\boldsymbol{\gamma}] [\sigma_{\bar{\beta}_0}^2] [\sigma_\eta^2].$$

232 Accomodating zeros

233 Our process model (in Eq. 2) includes a log transformation of the observations ($\log(y_{t-1})$).
 234 Thus, our model does not accomodate zeros. Fortunately, we had very few instances where
 235 pixels had 0% cover at time $t-1$ ($N = 47$, which is 0.01% of the data set). Thus, we ex-
 236 cluded those pixels from the model fitting process. However, when simulating the process,
 237 we needed to include possible transitions from zero to non-zero percent cover. We fit an
 238 intercept-only logistic model to estimate the probability of a pixel going from zero to non-
 239 zero cover

$$y_i \sim \text{Bernoulli}(\mu_i) \quad (8)$$

$$\text{logit}(\mu_i) = b_0 \quad (9)$$

241 where \mathbf{y} is a vector of 0s and 1s corresponding to whether a pixel was colonized ($>0\%$
 240 cover) or not (remains at 0% cover) and μ_i is the expected probability of colonization as
 242 a function of the mean probability of colonization (b_0). We fit this simple model using the
 243 ‘glm’ command in R (R Core Team 2013). For data sets in which zeros are more common
 244 and the colonization process more important, the same spatial statistical approach we used
 245 for our cover change model could be applied and covariates such as cover of neighboring cells
 246 could be included.
 247

Fitting the model

We fit the spatiotemporal model in R (R Core Team 2013) using the ‘No-U-Turn’ Hamiltonian Monte Carlo sampler in Stan (Stan Development Team 2014a) and the RStan package (Stan Development Team 2014b). We obtained posterior distributions of all model parameters from three MCMC chains comprised of 1,000 iterations each, after discarding an initial 1,000 iterations as burn in. Short chains of samples are a hallmark of the Stan algorithm, which is extremely efficient. Compared to other samplers, fewer iterations are required to achieve convergence. Each chain was initialized with unique parameter values and the model was fit in parallel using the Utah State University High-Performance Computing facility. Model fitting required five days on a four node Central Processing Unit with $2 \times$ AMD Opteron(tm) Processor 4386 @ 3.10 Ghz, 64GB of RAM per node, 16 cores per node, and each chain launched in parallel on separate cores. We assessed convergence visually and calculated scale-reduction factors (Appendix C, $\hat{R} < 1.1$ for all parameters) (Gelman and Rubin 1992, Gelman and Hill 2009).

Simulating the process

We performed four sets of simulations to (1) compare observed and simulated equilibrium cover, (2) compare observed and simulated year- and location-specific cover, (3) forecast future equilibrium population states under projected climate change, and (4) make temporally-explicit forecasts of sagebrush cover starting the final year of our observations and ending in year 2098. Using the posterior distribution of model parameters, we simulated a matrix of pixels equal to the size of the study area (13,689 pixels or matrix elements). For simulations (1) and (3) we initialized all pixels with arbitrarily low cover (1%) and then projected the model forward by randomly drawing climate covariates from the observed climate time series (for 1) or a perturbed climate time series (for 3). We ran equilibrium simulations (1 and 3) for 2,000 time steps and then compared the output across

simulations, after discarding an initial 100 time steps. To calculate average future equilibrium sagebrush cover, we ran simulation (3) for each GCM and RCP scenario separately, and then averaged the results over GCMs. For simulation (2), we initialized each pixel with its actual percent cover value for time t and cell s and projected the model forward one time step and compared the one-step ahead forecast with the observed value. For simulation (4), we initialized each pixel with the final observed value in 2011 and then projected the model forward based on GCM yearly weather projections. We ran these simulations for each GCM and RCP scenario combination separately and then aggregated the results over the GCMs by calculating the mean and the 90th percentiles for each RCP scenario.

We used the posterior mean of each parameter for all simulations except for (4) where we ran 50 simulations with unique sets of parameters from the chains. Random year effects were included in simulations by randomly drawing a posterior mean year effect ($\beta_{0,t}$) for each iteration (simulations 1 and 3), using the posterior mean year effect for a specific year (simulation 2), or by a drawing a future-year random effect from the posterior mean and standard deviation of the mean intercept (simulation 4, e.g., $\beta_{0,T} \sim \text{normal}(\bar{\beta}_0, \sigma_{\beta_0}^2)$ for some future year T). Our simulation approach provides a reasonable and computationally efficient approximation to the true posterior predictive mean when used in these scenarios with our data.

We required future projections of climate for our study area to conduct the equilibrium and temporally-explicit forecasts described above. Thus, we used the most recent climate projections from the Intergovernmental Panel on Climate Change (IPCC), the Coupled Model Intercomparison Project 5 (CMIP5; *available online*)². The CMIP5 provides projections from a suite of global circulations models (GCMs); we used projections from 18 GCMs (Table A1) that produced weather projections for three “Representative Concen-

²<http://cmip-pcmdi.llnl.gov/cmip5/>

tration Pathways”: RCP 4.5, RCP 6.0, and RCP 8.5 (*described online*)³. The three RCPs correspond to stabilization of radiative forcing before 2100, after 2100, and ongoing increase in greenhouse gas emissions, respectively.

To simulate equilibrium sagebrush cover under projected future climate we applied average projected changes in precipitation and temperature to the observed climate time series. For each GCM and RCP scenario combination, we calculated average precipitation and temperature over the 1950-2000 time period and the 2050-2098 time period. We then calculated the absolute change in temperature between the two time periods (ΔT) and the proportional change in precipitation between the two time periods (ΔP) for each GCM and RCP scenario combination. Lastly, we applied ΔT and ΔP to the observed 28-year climate time series to generate a future climate time series for each GCM and RCP scenario combination. These generated climate time series were used to simulate equilibrium sagebrush cover. We simulated equilibrium cover separately for each GCM and RCP scenario combination before averaging the results, but we show the average projected climate changes across all models in Table 1.

For the temporally-explicit forecasts we used yearly GCM projections from 2012 to 2098 to simulate the process starting from the end point of the remotely sensed sagebrush cover data (ends in 2011). We aggregated daily GCM output for each GCM and RCP scenario into the seasonal climate covariates used to fit our model. These yearly climate time series were not aggregated further because we ran simulations for each GCM and RCP scenario, rather than one simulation per RCP scenario averaged over GCMs. **Note that forecasting with our model, which relies on historical correlations between sagebrush cover change and weather, using future climate projections requires assuming such relationships remain in the future.**

³<http://tntcat.iiasa.ac.at/RcpDb/>

Results

Averaging across all GCMs, precipitation and temperature in our study area are projected to increase; the magnitude of increase depends on the RCP scenario (Table 1). Trajectories of our climate covariates from GCM projections show similar trends (Fig. 2).

All parameters in our model converged on stable posterior distributions (Appendix C). Only the *lagPpt* climate covariate can be considered important based on a 90% credible interval, and it had a positive effect on sagebrush percent cover change (Fig. 3). In other words, if the year 2000 water year was wetter than average, sagebrush cover would increase from the 2001 to the 2002 growing season. Other climate effects strongly overlapped zero but their posterior means were positive, except for fall-through-spring precipitation the first year of a cover transition ($t-1$), whose posterior mean was negative (Fig. 3). The posterior mean for the spatial random effect, η , captured the overall spatial structure of the observed data (Fig. D1). This indicates our choice of knot placement and dimension reduction strategy was adequate for describing permanent spatial variation in the data.

When we simulated the pixel-based population model based on observed climate, it was able to reproduce the spatial pattern of observed percent cover, averaged over time (Fig. 4A,B). Our model shows a tendency to underpredict perennially-low percent cover pixels (Fig. 4C), but does a better job at predicting high cover pixels. Point predictions are most confident, though slightly biased, in low percent cover pixels (Fig. 4D). The model is also able to adequately reproduce observed dynamics when we make one-step-ahead predictions based on observed climate and cover in the previous year for each pixel. When we made these in-sample, one-step-ahead forecasts, the model achieved an $\text{RMSE} = 4.31$, in units of percent cover. The Pearson's correlation between observations and predictions was 0.62.

When we apply the fitted model to IPCC climate change scenarios, the model predicts gains in sagebrush percent cover, on average (Figs. 5, 6). The spatial effect remains strong enough in low cover regions to counteract the positive effect of projected precipitation

increases (Fig. 5). Thus, our model predicts an increase in the heterogeneity of sagebrush cover because projected cover increases are smaller in low cover pixels than in high cover pixels (Fig. 5 and Fig. E1). For the temporally-explicit forecasts, we show spatially-averaged values and the associated uncertainty due to variability in GCM projections, variability in model parameters, and uncertainty in our process model (Fig. 6). Based on our model and GCM projections, we forecast an average increase in sagebrush cover at our study area, but a decrease is not outside the realm of possibility (shaded regions in Fig. 6). The generally increasing trend reflects the positive effect of precipitation on sagebrush cover change estimated for our study area (Fig. 3).

Discussion

Despite the need to forecast population responses to climate change over large spatial extents, as demonstrated by the wide application of species distribution models (e.g., Clark et al. 2014), landscape-scale population models for plant species remain more concept than reality (Schurr et al. 2012, Merow et al. 2014). We introduced a new approach that combines a remotely-sensed time series of plant percent cover (Homer et al. 2012) and methods from the spatio-temporal modeling literature (e.g., Conn et al. 2015). As a proof-of-concept, we applied our approach to a remotely-sensed data product of sagebrush percent cover from 1984 to 2011 in Wyoming. We first discuss our results specific to sagebrush ecology and response to climate, and then discuss the more general implications and limitations of our proposed approach.

Sagebrush response to climate and climate change

The climate effects we estimated, based on cover data at 30 meter spatial resolution, are consistent with individual-level responses of sagebrush to climate-related variables. Research on individual plants has shown that wetter winters are correlated with greater stem

growth in sagebrush (Poore et al. 2009, Apodaca 2013) and that warmer spring temperatures may enhance sagebrush growth in cold climates by advancing the date of snowmelt and increasing the length of the growing season (Perfors et al. 2003, Harte et al. 2015). In agreement with those individual-level responses, posterior means for all precipitation and temperature effects in our model were positive, except for the effect of fall-through-spring precipitation in the first year of a cover transition (*ppt1*, Fig. 3). The cumulative amount of precipitation the year before a cover transition (*pptLag* in our model) emerged as the strongest predictor of sagebrush cover change (Fig. 3). However, mean estimates for the climate effects are relatively weak (Fig. 3). Such small effects could indicate that sagebrush are not very sensitive to interannual climate variability, that our model is poorly specified, or that climate responses are difficult to detect using coarse-scale data. Given findings from previous research demonstrating the importance of precipitation and temperature to sagebrush growth (Pechanec et al. 1937, Schlaepfer et al. 2011, Germino and Reinhardt 2014) and regeneration (Schlaepfer et al. 2014b), it is unlikely that sagebrush are insensitive to climate. We used aggregated climate covariates that may not completely capture the climate-dependence of sagebrush cover change. However, the covariates we chose closely match the climate-related variables that have been shown to drive sagebrush growth, survival, and regeneration (e.g., Dalglish et al. 2011, Schlaepfer et al. 2014b). More likely, aggregated estimates of plant abundance, such as percent cover, mask interannual variability at the level of the individual plant and makes it more difficult to detect the drivers of interannual variability. Additionally, we chose not to downscale the Daymet weather data, meaning that in a given year all pixels shared the same climate, which limits our statistical power. Nonetheless, our model was capable of detecting climate effects that agree with our knowledge of sagebrush ecology and allowed us to make forecasts of future sagebrush abundance.

Under projected climate, we forecast modest increases in sagebrush cover for all RCP scenarios (Figs. 5,6). Our forecasts reflect both the estimated effect size for each climate co-

variate and the amount of change in those covariates projected by the GCMs. Cumulative precipitation the year before a given year-to-year transition was the strongest standardized effect (Fig. 3), but precipitation is projected to increase only moderately (Table 1, Fig. 2) and the negative effect of fall-through-spring precipitation in the first year of a cover transition (*ppt1*) had an offsetting effect. In contrast, mean spring temperature had a weak positive effect on sagebrush cover changes, but the projected temperature increase is large (Table 1, Fig. 2).

An interesting consequence of explicitly modeling the effect of space (through η) is the forecasted increase in spatial heterogeneity (Fig. E1). Our model projects little change in low cover pixels but substantial increases in the cover of high cover pixels (Fig. 5). Had we not explicitly accounted for spatial-dependence in our model, we would have missed this result. We were unable to attribute the spatial structure apparent in the data (Fig. 4A) and approximated by our model (η , Fig. D1) to slope, aspect, elevation, or coarse soil type (results not shown). The lack of correlation between η and landscape factors leads us to conclude that the spatial structure in our data set emerges from some combination of fine-scale microhabitat associations and legacy effects related to fire and species invasions.

While we forecast an increase in sagebrush cover at our study area, SDM studies typically project dramatic declines in climate suitability for sagebrush with warming (Shafer et al. 2001, Neilson et al. 2005, Bradley 2010, Schlaepfer et al. 2012, Still and Richardson 2015). There are many potential explanations for this apparent contrast, ranging from the type of model used to the particular climate covariates considered, but the location of our study area in a cold portion of sagebrush's geographic distribution may be the best. The response of plant species to weather varies along climatic gradients (e.g., Clark et al. 2011, Vanderwel et al. 2013), and sagebrush are especially sensitive to the timing of snowmelt because their growth depends on recharge of deep soil water (Schlaepfer et al. 2012, Schlaepfer et al. 2014a). In warmer parts of the sagebrush range, earlier snowmelt is detrimental to growth and survival (Pechanec et al. 1937, Schlaepfer et al. 2011, Germino

and Reinhardt 2014). In colder regions, earlier snowmelt due to temperature increases can lengthen the growing season and increase sagebrush occurrence and cover (Schlaepfer et al. 2012, Schlaepfer et al. 2014a). The average annual temperature across the sagebrush steppe biome is 6.9°C (sd = 1.6; Schlaepfer et al. 2011), whereas average temperature at our study area from 1980 to 2013 was 4.6°C (calculated from Daymet estimates). Our study area lies at the cold extreme of the sagebrush range, thus the weak positive response to temperature that we estimated (Fig. 3) and carried through to our forecasts (Figs. 5,6) likely represents the positive effect of earlier snowmelt, and thus higher moisture availability early in the growing season.

A previous analysis of a different subset of the remote sensing data set we used also came to a different conclusion, projecting future sagebrush decline (Homer et al. 2015). The discrepancy between the results of Homer et al. (2015) and ours primarily reflects a difference in the climate projections used for projecting future changes rather than differences in our inference about responses to historical variation in weather. Homer et al. (2015) used downscaled weather projections from a single model from the IPCC 4 whereas we used native-resolution weather projections from a suite of models from the IPCC 5. Consistent with our study, Homer et al. (2015) found a generally positive relationship between pixel-level sagebrush cover and precipitation, but the future climate scenario they chose resulted in a mean decrease in precipitation, causing a predicted decline in sagebrush cover. A second difference is that Homer et al. (2015) relied on regressions of decadal trends in sagebrush cover against decadal trends in climate at the level of individual pixels. Our current approach is fundamentally different in that we specifically model the impact of interannual variation in weather on year-to-year changes in sagebrush cover using a dynamic population model. Thus, our model takes advantage of the additional information contained within short-term responses to climate fluctuations. Lastly, the location of Homer et al.'s (2015) study area is, on average, at a lower elevation than our current study area. The geographic difference results in different historical and projected climate, and, as dis-

cussed above, sagebrush may respond differently to warming depending on geographic location.

We projected sagebrush cover to the end of this century, but an important feature of our approach is that it could also produce short-term forecasts. For example, we could forecast the effects of a multi-year regional drought on sagebrush cover (Debinski et al. 2010). Validating spatial population models against short-term predictions would give ecological forecasters a way to assess and improve the performance of their models, which would greatly increase our confidence in long-term forecasts. This cycle of prediction, validation, and refinement is missing from most currently available population-level forecasts of the effects of climate change.

A landscape-scale plant population modeling approach: opportunities and limitations

Our approach for modeling plant populations overcomes two major hurdles for spatially-explicit population models. First, we used moderate resolution, remotely-sensed estimates of sagebrush percent cover as a response variable, enabling us to fit a dynamic population model over a large spatial extent. Species-specific estimates of plant abundance are becoming commonplace as remote sensing technology develops (e.g., Baldeck and Asner 2014, Colgan and Asner 2014), and in a few years several remotely-sensed time series may be available. Second, borrowing from new methods in spatio-temporal modeling of animal abundance (e.g., Conn et al. 2015), we fit the model using a dimension reduction strategy that accounted for spatial autocorrelation within a feasible computational time. Accounting for spatial autocorrelation allows for statistically rigorous inference on the effects of interannual climate on sagebrush cover change in our study region. The spatial covariance structure also provided a way to obtain spatially-explicit predictions at a resolution below that of the climate covariates (i.e., within the study region; Figs. 4,5). Our approach is amenable to any

spatially-explicit time series of plant abundance, but we see remote-sensing datasets offering the largest opportunity for landscape-scale population models. Furthermore, it would be straightforward to include additional covariates related to disturbance (e.g., fire) or biotic interactions. Thus, we see our method as a first step toward coupling the mechanistic power of dynamic population models with the spatial extent of SDMs. The spatially- and temporally-explicit forecasts made possible by our approach should be especially relevant to land management decisions based on near-term forecasts.

Several *a priori* modeling decisions determined the spatial extent and resolution of our results. We retained the native spatial resolution of the remote sensing data (30×30 meters). This constrained the extent that we could reasonably model because of the computational challenges in estimating spatial random effects. Even with our dimension reduction technique, modeling a larger area at this resolution would require a greater number of spatial knots, and computation time would increase substantially (Wikle 2010). To model a larger spatial extent, we could aggregate the original remote-sensing time series data to a coarser spatial resolution. This would allow us to model a much greater spatial extent with a similar number of knots and a similar computation time. While a coarser scale model would lose some fine-scale detail, it could be applied to a much larger area, potentially gaining some strength in estimating climate effects by spanning a greater range of climate variation. However, gains made by incorporating greater regional variability by modeling at a coarser resolution could be offset by the loss of information inherent when aggregating plant responses into larger pixels.

Our spatial extent and resolution also affected our use of climate covariates. We did not downscale Daymet data to match the spatial resolution of the sagebrush data, meaning that in each year all pixels share the same climate covariates. This is a potential limitation of our study, and could explain the weak effect of climate covariates that we observed (Fig. 3). We also did not allow different portions of our study area to respond to climate in different ways. Doing so would require spatially-varying climate effects and a substan-

tial increase in computational time. However, in future applications, it will be important to allow climate effects to vary over space to better capture reality. Conn et al. (2015) provide examples of how such spatiotemporal interactions can be included in abundance models. We might expect climate effects to interact with spatial covariates such as soil type, slope, and aspect. In our relative small study area, we did not observe important effects of these factors, but it is possible to include such abiotic data layers as predictors when fitting models at larger spatial extents where variability may be greater.

The uncertainty associated with our forecasts highlights several opportunities to improve our approach. First, parameter uncertainty could be reduced by regulating the variance of the posterior distributions of climate covariates via ridge regression (e.g., Gerber et al. 2015). Second, uncertainty associated with climate projections could be reduced by identifying GCMs that perform exceptionally well for a particular study location (e.g., Rupp et al. 2013). Such considerations will be important when forecasting in support of particular management objectives.

Conclusion

We introduced a new approach to fitting and simulating population models at large spatial extents with plant population data derived from state of the art remote sensing. We used the model to forecast future abundances of sagebrush in Wyoming and found that at our relatively cold site sagebrush should be expected to increase in cover. As more species-level remote sensing datasets become available and computing power increases this approach will be applicable to a wider number of species and even larger spatial extents. Future modeling could include the effects of non-climate drivers – including the effects of species interactions and disturbance. For sagebrush, including fire and competition with non-native annual grasses in the model may be especially important for a complete assessment of the effects of climate change (Bradford and Lauenroth 2006). Fortunately, our

spatio-temporal modeling framework could easily be extended to model additional species and dynamic processes as the data become available. The approach we have developed here fills an important gap in spatial scales between species distribution models and local-scale demographic population models.

Acknowledgments

This work is the outcome of a distributed graduate seminar led by PBA and supported by a National Science Foundation CAREER award (DEB-1054040). David T. Iles, Eric LaMalfa, and Rebecca Mann participated in project conception as part of the distributed graduate seminar and provided comments that improved the manuscript. ATT was supported by an NSF Postdoctoral Research Fellowship in Biology (DBI-1400370) and AK was supported by an NSF Graduate Research Fellowship. Additional support came from the Utah Agricultural Experiment Station, Utah State University, and this article is approved as journal paper number 8856. We are grateful to Debra K. Meyer at USGS EROS for extracting the data set used in this paper and to David Koons for comments that improved the manuscript. Compute, storage, and other resources from the Division of Research Computing in the Office of Research and Graduate Studies at Utah State University are gratefully acknowledged. We acknowledge the World Climate Research Programme’s Working Group on Coupled Modelling, which is responsible for CMIP, and we thank the climate modeling groups (listed in Table A1) for producing and making available their model output. For CMIP the U.S. Department of Energy’s Program for Climate Model Diagnosis and Intercomparison provides coordinating support and led development of software infrastructure in partnership with the Global Organization for Earth System Science Portals. Any use of trade, firm, or product names is for descriptive purposes only and does not imply endorsement by the U.S. government.

Table 1: Projected changes in temperature and precipitation at our study area from CMIP5 average GCM projections for 2050-2100 relative to average temperature and precipitation from 1950-2000.

Emissions Scenario	Absolute change in temperature	Percentage change in precipitation
RCP 4.5	2.98°	8.94%
RCP 6.0	3.13°	8.64%
RCP 8.5	4.79°	11.0%

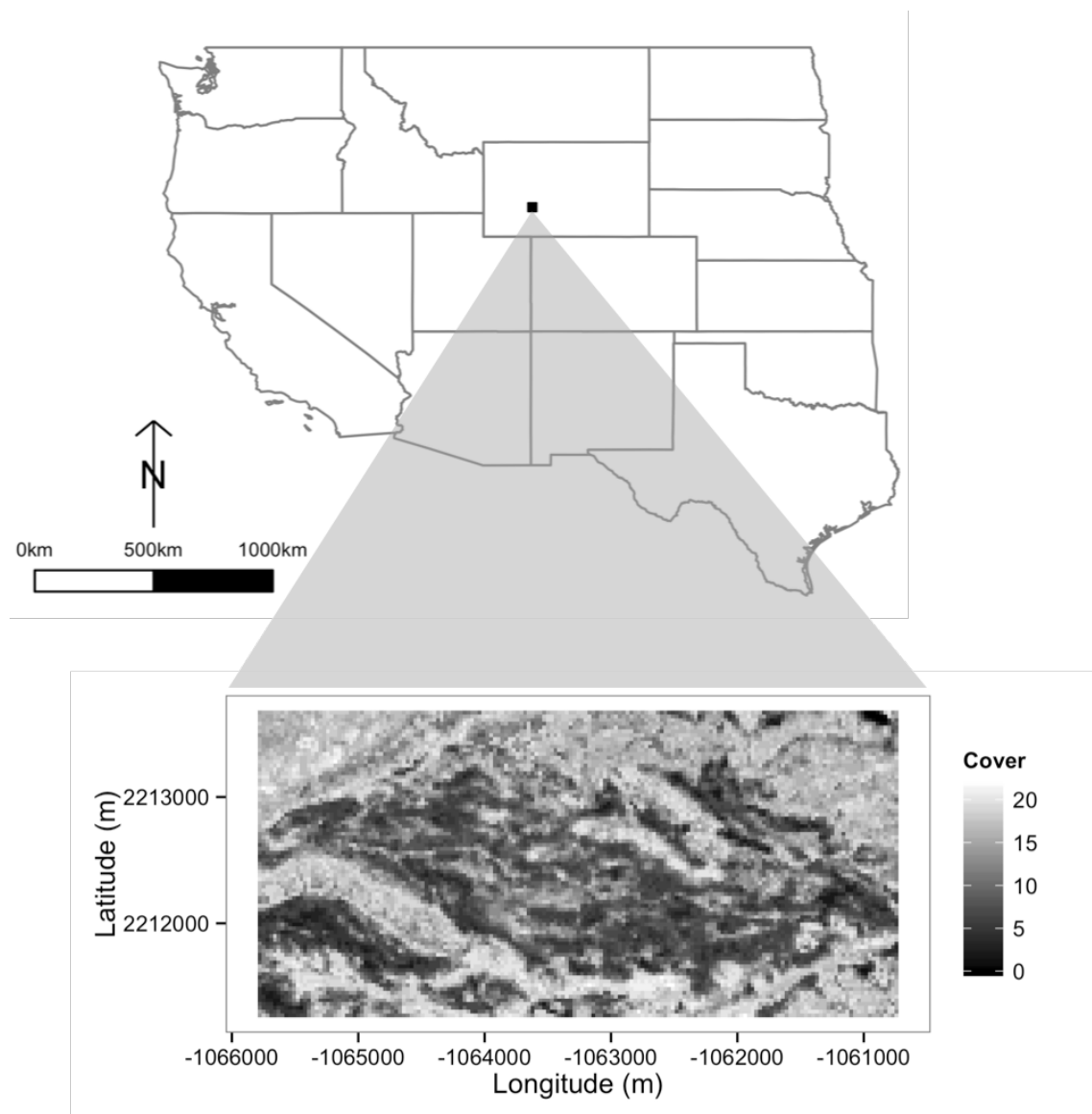


Figure 1: Location of the $5,070 \times 2,430$ meter study area in southwestern Wyoming (black rectangle) and a snapshot of the percent cover data in 1984 (detailed inset). Scale bar is relevant for US map only; refer to axes labels on the detailed inset of sagebrush percent cover for scale of the study area.

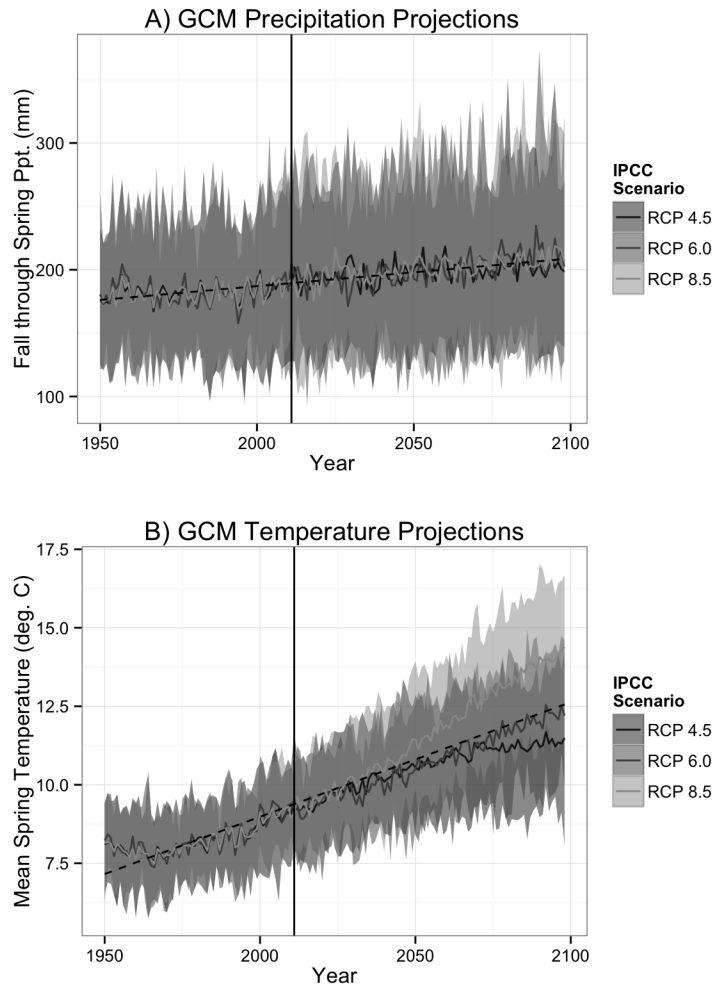


Figure 2: GCM yearly weather hindcasts (before solid line at 2011) and projections (after solid line at 2011) for precipitation (A) and temperature (B) at our study area in southwestern Wyoming (see Fig. 1).

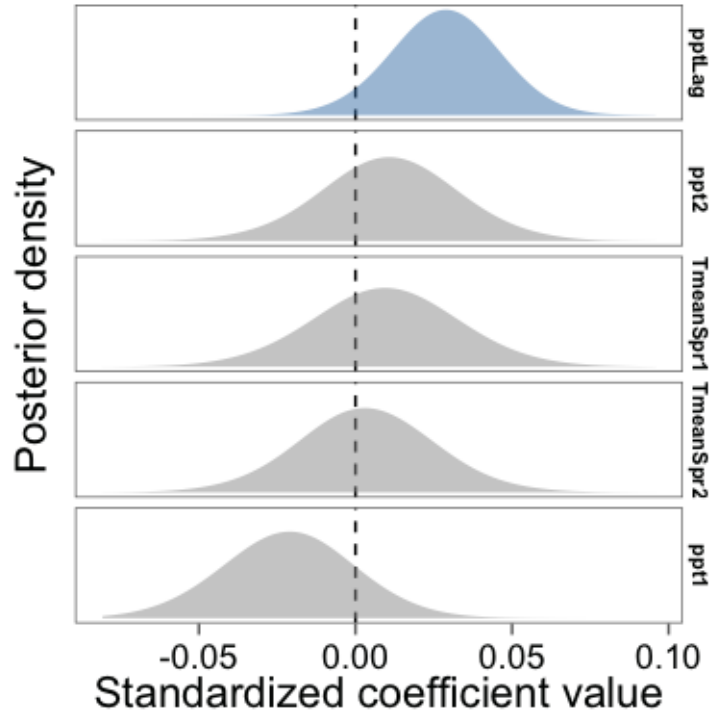


Figure 3: Posterior distributions of climate covariates. The x-axis is the standardized coefficient value because we fit the statistical model for sagebrush cover change (Eq. 7) using standardized covariate values. Only cumulative precipitation at time $t-2$ (pptLag) is important (shown in blue; 90% CI does not overlap zero). Climate covariate codes: pptLag = water year precipitation in year $t-2$; TmeanSpr1 = year $t-1$ average spring temperature; ppt2 = year t fall through summer precipitation; TmeanSpr2 = year t average spring temperature; ppt1 = year $t-1$ fall through summer precipitation.

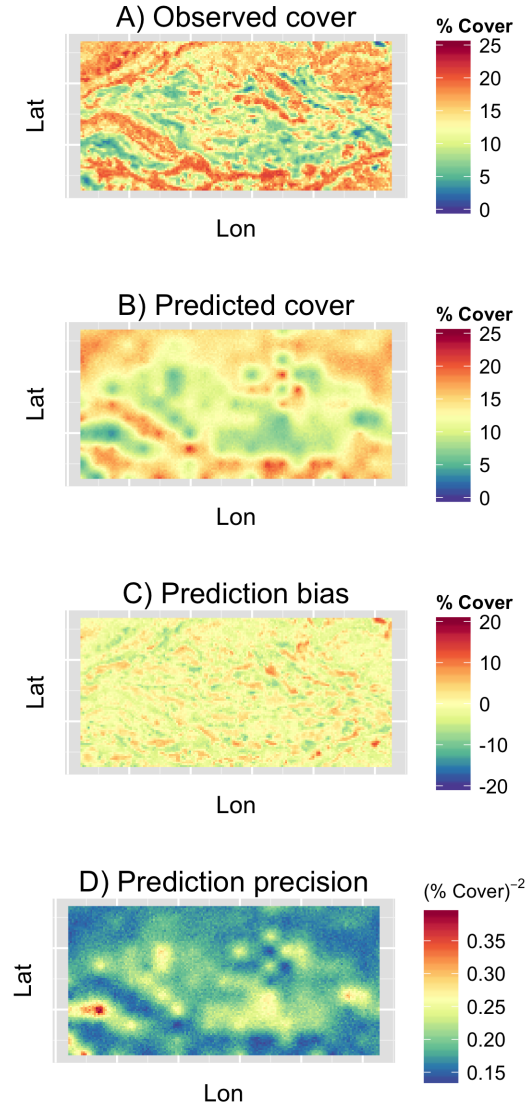


Figure 4: Observed and predicted (A, B) equilibrium percent cover of sagebrush, and prediction bias and precision (C, D) for the extent of our spatial area at 30-m resolution. Observed equilibrium sagebrush cover (A) is the temporal mean of each pixel from the 28 year time series. Prediction results are from simulations that use posterior mean parameter values. Precision in (D) represents the variability of each pixel over the course of the 2,000 iteration simulation. Axes definitions: Lat = latitude; Lon = longitude.

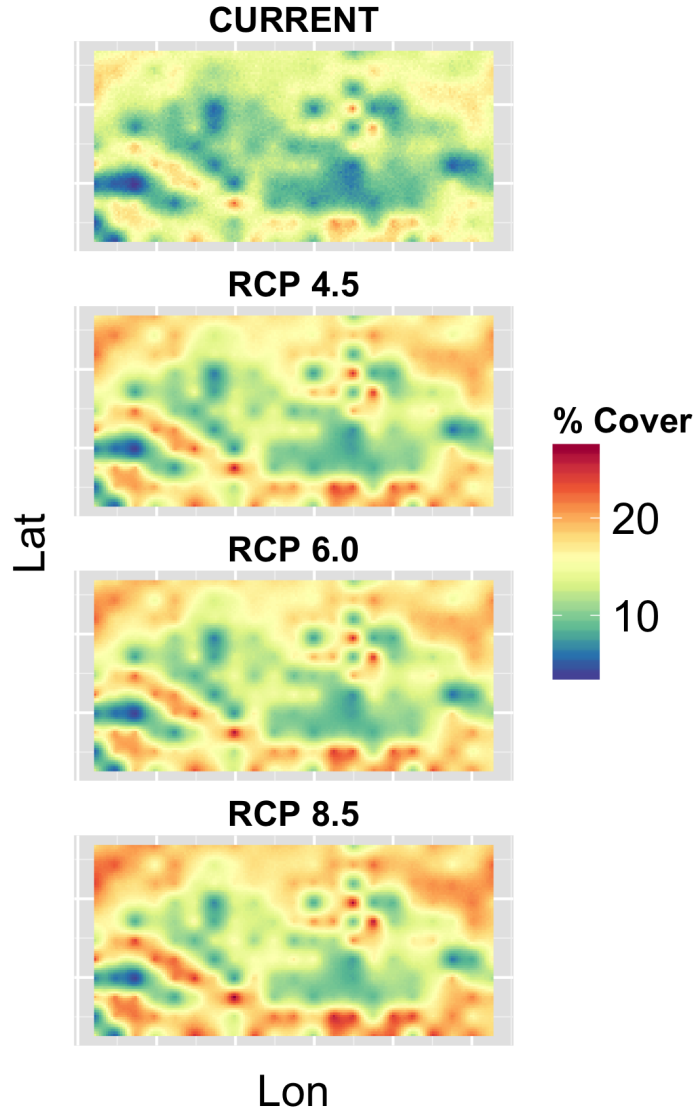


Figure 5: Projected equilibrium cover under three IPCC climate change scenarios (RCP = Representative Concentration Pathways) for our study area in southwestern Wyoming. The top panel shows equilibrium cover based on simulations using observed climate. Subsequent panels show equilibrium cover based on perturbed climate for each RCP scenario. Forecasts are based on the projected climate changes in Table 1 applied to the observed climate time series used to fit the statistical model. We used posterior mean parameter estimates for all simulations. Color bar indicates percent cover of sagebrush in each 30x30 meter pixel. Axes definitions: Lat = latitude; Lon = longitude.

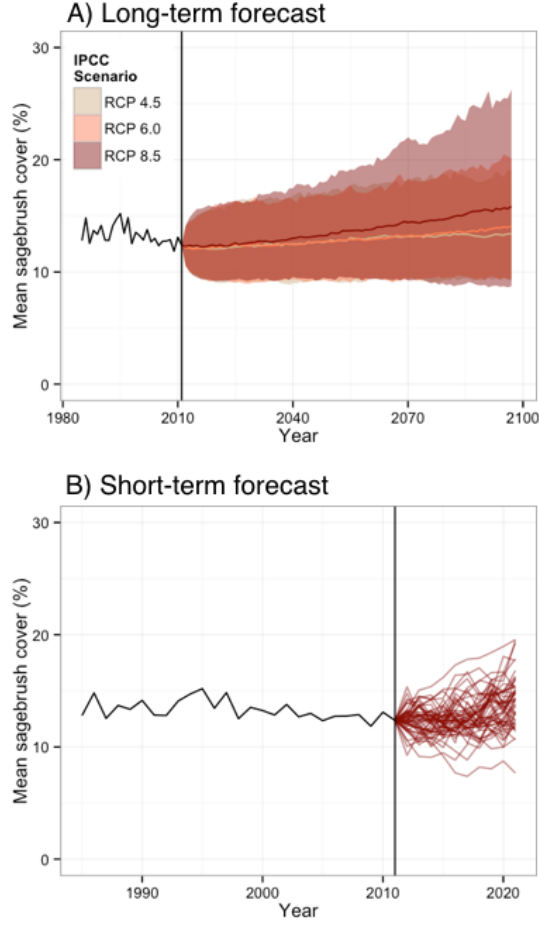


Figure 6: Observed (black line before 2011) and forecasted (colored lines after 2011) sagebrush percent cover. Long-term forecasts (A) were made for three IPCC emissions scenarios (RCPs 4.5, 6.0, and 8.5) and are for the period of 2012 to 2098. Shaded regions show limits of the 5th and 95th quantiles for simulations conducted using 50 different sets of parameters from the MCMC output. Lines show mean trajectories. Uncertainty in forecasts arises from uncertainty in GCM projections, uncertainty around the ecological process, and uncertainty around parameter estimates. Before calculating the mean and quantiles for each year across parameter sets and GCMs, we averaged percent cover over the 13,689 pixels. Panel (B) shows an example short-term forecast (10 years) using the MIROC5 GCM projections under RCP 8.5. Each line shows a forecast from one parameter set.

References

- Adler, P. B., H. J. Dalglish, and S. P. Ellner. 2012. Forecasting plant community impacts of climate variability and change: when do competitive interactions matter? *Journal of Ecology* 100:478–487.
- Apodaca, L. F. 2013. Assessing Growth Response to Climate Controls in a Great Basin *Artemisia Tridentata* Plant Community. PhD thesis, University of Nevada Las Vegas.
- Arnett, E. B., and T. Z. Riley. 2015. Science, policy, and the fate of the greater sage-grouse. *Frontiers in Ecology and the Environment* 13:235.
- Baldeck, C. A., and G. P. Asner. 2014. Improving remote species identification through efficient training data collection. *Remote Sensing* 6:2682–2698.
- Barry, R. P., and J. M. V. Hoef. 1996. Blackbox Kriging: Spatial Prediction without Specifying Variogram Models.
- Bradford, J. B., and W. K. Lauenroth. 2006. Controls over invasion of *Bromus tectorum*: The importance of climate, soil, disturbance, and seed availability. *Journal of Vegetation Science* 17:693–704.
- Bradley, B. A. 2010. Assessing ecosystem threats from global and regional change: hierarchical modeling of risk to sagebrush ecosystems from climate change, land use and invasive species in Nevada, USA. *Ecography* 33:198–208.
- Clark, J. S., D. M. Bell, M. H. Hersh, and L. Nichols. 2011. Climate change vulnerability of forest biodiversity: Climate and competition tracking of demographic rates. *Global Change Biology* 17:1834–1849.
- Clark, J. S., S. R. Carpenter, M. Barber, S. Collins, A. Dobson, J. A. Foley, D. M. Lodge, M. Pascual, R. Pielke, W. Pizer, C. Pringle, W. V. Reid, K. A. Rose, O. Sala, W. H. Schlesinger, D. H. Wall, and D. Wear. 2001. Ecological forecasts: an emerging imperative. *Science (New York, N.Y.)* 293:657–660.

581 Clark, J. S., A. E. Gelfand, C. W. Woodall, and K. Zhu. 2014. More than the sum of the
 582 parts: Forest climate response from joint species distribution models. *Ecological Applica-*
 583 *tions* 24:990–999.

584 Colgan, M. S., and G. P. Asner. 2014. Coexistence and environmental filtering of species-
 585 specific biomass in an African savanna. *Ecology* 95:1579–1590.

586 Conn, P. B., D. S. Johnson, J. M. V. Hoef, M. B. Hooten, J. M. London, and P. L. Boveng.
 587 2015. Using spatiotemporal statistical models to estimate animal abundance and infer
 588 ecological dynamics from survey counts. *Ecological Monographs* 85:235–252.

589 Dalglish, H. J., D. N. Koons, M. B. Hooten, C. A. Moffet, and P. B. Adler. 2011. Climate
 590 influences the demography of three dominant sagebrush steppe plants. *Ecology* 92:75–85.

591 Debinski, D. M., H. Wickham, K. Kindscher, J. C. Caruthers, and M. Germino. 2010.
 592 Montane meadow change during drought varies with background hydrologic regime and
 593 plant functional group. *Ecology* 91:1672–81.

594 Ehrlén, J., and W. F. Morris. 2015. Predicting changes in the distribution and abundance
 595 of species under environmental change. *Ecology Letters* 18:303–314.

596 Elith, J., and J. R. Leathwick. 2009. *Species Distribution Models: Ecological Explanation*
 597 *and Prediction Across Space and Time*.

598 Ellner, S. P., and M. Rees. 2006. Integral projection models for species with complex de-
 599 mography. *The American naturalist* 167:410–428.

600 Freckleton, R. P., W. J. Sutherland, A. R. Watkinson, and S. A. Queenborough. 2011.
 601 Density-structured models for plant population dynamics. *American Naturalist* 177:1–17.

602 Gelman, A., and J. Hill. 2009. *Data analysis using regression and multilevel/hierarchical*
 603 *models*. Cambridge University Press, Cambridge.

604 Gelman, A., and D. B. Rubin. 1992. Inference from Iterative Simulation Using Multiple
 605 Sequences. *Statistical Science* 7:457–472.

606 Gerber, B. D., W. L. Kendall, M. B. Hooten, J. A. Dubovsky, and R. C. Drewien. 2015.
 607 Optimal population prediction of sandhill crane recruitment based on climate-mediated
 608 habitat limitations. *Journal of Animal Ecology* 84:1299–1310.

609 Germino, M. J., and K. Reinhardt. 2014. Desert shrub responses to experimental modifi-
 610 cation of precipitation seasonality and soil depth: Relationship to the two-layer hypothesis
 611 and ecohydrological niche. *Journal of Ecology* 102:989–997.

612 Hare, J. a, M. a Alexander, M. J. Fogarty, E. H. Williams, and J. D. Scott. 2010. Fore-
 613 casting the dynamics of a coastal fishery species using a coupled climate–population model.
 614 *Ecological applications* : a publication of the Ecological Society of America 20:452–464.

615 Harte, J., S. R. Saleska, and C. Levy. 2015. Convergent ecosystem responses to 23-year
 616 ambient and manipulated warming link advancing snowmelt and shrub encroachment to
 617 transient and long-term climate-soil carbon feedback. *Global change biology* 21:2349–56.

618 He, K. S., B. A. Bradley, A. F. Cord, D. Rocchini, M.-N. Tuanmu, S. Schmidtlein, W.
 619 Turner, M. Wegmann, and N. Pettorelli. 2015. Will remote sensing shape the next genera-
 620 tion of species distribution models? *Remote Sensing in Ecology and Conservation* 1:4–18.

621 Higdon, D. 1998. A process-convolution approach to modelling temperatures in the North
 622 Atlantic Ocean. *Environmental and Ecological Statistics* 5:173–190.

623 Higdon, D. M. 2002. Space and space-time modeling using process convolutions. Pages
 624 37–56 *in* C. Anderson, V. Barnett, P. Chatwin, and A. El-Shaarawi, editors. *Quantitative*
 625 *methods for current environmental issues*. Springer, London.

626 Hobbs, N. T., and M. B. Hooten. 2015. *Bayesian Models: A Statistical Primer for Ecolo-*
 627 *gists*. Princeton University Press, Princeton.

628 Homer, C. G., C. L. Aldridge, D. K. Meyer, and S. J. Schell. 2012. Multi-scale remote
 629 sensing sagebrush characterization with regression trees over Wyoming, USA: Laying a
 630 foundation for monitoring. *International Journal of Applied Earth Observation and Geoin-*

formation 14:233–244.

Homer, C. G., G. Xian, C. L. Aldridge, D. K. Meyer, T. R. Loveland, and M. S.

O'Donnell. 2015. Forecasting sagebrush ecosystem components and greater sage-grouse

habitat for 2050: Learning from past climate patterns and Landsat imagery to predict the

future. *Ecological Indicators* 55:131–145.

Hooten, M. B., and N. T. Hobbs. 2015. A guide to Bayesian model selection for ecologists.

Ecological Monographs 85:3–28.

Hooten, M. B., and C. K. Wikle. 2007. Shifts in the spatio-temporal growth dynamics of

shortleaf pine. *Environmental and Ecological Statistics* 14:207–227.

Hooten, M. B., D. R. Larsen, and C. K. Wikle. 2003. Predicting the spatial distribution

of ground flora on large domains using a hierarchical Bayesian model. *Landscape Ecology*

18:487–502.

Kuchler, A. 1964. Potential Natural Vegetation of the Conterminous United States. Ameri-

can Geographical Society, Special Publication No. 36.

Latimer, A. M., S. Banerjee, H. Sang, E. S. Mosher, and J. A. Silander. 2009. Hierarchical

models facilitate spatial analysis of large data sets: A case study on invasive plant species

in the northeastern United States. *Ecology Letters* 12:144–154.

Luo, Y., K. Ogle, C. Tucker, S. Fei, C. Gao, S. LaDeau, J. S. Clark, and D. S. Schimel.

2011. Ecological forecasting and data assimilation in a data-rich era. *Ecological Applica-*

tions 21:1429–1442.

Maiorano, L., R. Cheddadi, N. E. Zimmermann, L. Pellissier, B. Petitpierre, J. Pottier, H.

Laborde, B. I. Hurdu, P. B. Pearman, A. Psomas, J. S. Singarayer, O. Broennimann, P.

Vittoz, A. Dubuis, M. E. Edwards, H. A. Binney, and A. Guisan. 2013. Building the niche

through time: using 13,000 years of data to predict the effects of climate change on three

tree species in Europe. *Global Ecology and Biogeography* 22:302–317.

Merow, C., A. M. Latimer, A. M. Wilson, S. M. McMahon, A. G. Rebelo, and J. A. Silander. 2014. On using integral projection models to generate demographically driven predictions of species' distributions: development and validation using sparse data. *Ecography* 37:1167–1183.

Miglia, K., E. McArthur, W. Moore, H. Wang, J. Graham, and D. Freeman. 2005. Nine-year reciprocal transplant experiment in the gardens of the basin and mountain big sagebrush (*Artemisia tridentata*: Asteraceae) hybrid zone of Salt Creek Canyon: the importance of multiple-year tracking of fitness Title. *Biological Journal of the Linnean Society*:213–225.

Neilson, R., J. Lenihan, D. Bachelet, and R. Drapek. 2005. Climate change implications for sagebrush ecosystems. Page 145 *in* North american wildlife and natural resources conference.

Pechanec, J., G. Pickford, and G. Stewart. 1937. Effects of the 1934 Drought on Native Vegetation of the Upper Snake River Plans, Idaho. *Ecology*:490–505.

Perfors, T., J. Harte, and S. E. Alter. 2003. Enhanced growth of sagebrush (*Artemisia tridentata*) in response to manipulated ecosystem warming. *Global Change Biology* 9:736–742.

Petchey, O. L., M. Pontarp, T. M. Massie, S. Kéfi, A. Ozgul, M. Weilenmann, G. M. Palamara, F. Altermatt, B. Matthews, J. M. Levine, D. Z. Childs, B. J. McGill, M. E. Schaepman, B. Schmid, P. Spaak, A. P. Beckerman, F. Pennekamp, and I. S. Pearse. 2015. The ecological forecast horizon, and examples of its uses and determinants. *Ecology Letters* 18:597–611.

Poore, R. E., C. A. Lamanna, J. J. Ebersole, and B. J. Enquist. 2009. Controls on Radial Growth of Mountain Big Sagebrush and Implications for Climate Change. *Western North American Naturalist* 69:556–562.

Queenborough, S. A., K. M. Burnet, W. J. Sutherland, A. R. Watkinson, and R. P. Freck-

682 leton. 2011. From meso- to macroscale population dynamics: A new density-structured
683 approach. *Methods in Ecology and Evolution* 2:289–302.

684 R Core Team. 2013. R: A language and environment for statistical computing.

685 Rees, M., and S. P. Ellner. 2009. Integral projection models for populations in temporally
686 varying environments. *Ecological Monographs* 79:575–594.

687 Roberts, D. R., and A. Hamann. 2012. Predicting potential climate change impacts with
688 bioclimate envelope models: A palaeoecological perspective. *Global Ecology and Biogeog-*
689 *raphy* 21:121–133.

690 Ross, B. E., M. B. Hooten, J.-M. DeVink, and D. N. Koons. 2015. Combined effects of
691 climate, predation, and density dependence on Greater and Lesser Scaup population dy-
692 namics. *Ecological Applications* 25:1606–1617.

693 Running, S. W., R. R. Nemani, F. A. Heinsch, M. Zhao, M. Reeves, and H. Hashimoto.
694 2004. A Continuous Satellite-Derived Measure of Global Terrestrial Primary Production.
695 *BioScience* 54:547.

696 Rupp, D. E., J. T. Abatzoglou, K. C. Hegewisch, and P. W. Mote. 2013. Evaluation of
697 CMIP5 20th century climate simulations for the Pacific Northwest US. *Journal of Geo-*
698 *physical Research* 118:1–23.

699 Salguero-Gómez, R., O. R. Jones, C. R. Archer, Y. M. Buckley, J. Che-Castaldo, H.
700 Caswell, D. Hodgson, A. Scheuerlein, D. A. Conde, E. Brinks, H. de Buhr, C. Farack,
701 F. Gottschalk, A. Hartmann, A. Henning, G. Hoppe, G. Römer, J. Runge, T. Ruoff, J.
702 Wille, S. Zeh, R. Davison, D. Vieregg, A. Baudisch, R. Altwegg, F. Colchero, M. Dong,
703 H. de Kroon, J.-D. Lebreton, C. J. E. Metcalf, M. M. Neel, I. M. Parker, T. Takada, T.
704 Valverde, L. A. Vélez-Espino, G. M. Wardle, M. Franco, and J. W. Vaupel. 2015. The
705 compadrePlant Matrix Database: an open online repository for plant demography. *Journal*
706 *of Ecology* 103:202–218.

707 Schlaepfer, D. R., W. K. Lauenroth, and J. B. Bradford. 2011. Ecohydrological niche of
708 sagebrush ecosystems. *Ecohydrology*:n/a–n/a.

709 Schlaepfer, D. R., W. K. Lauenroth, and J. B. Bradford. 2014a. Modeling regeneration re-
710 sponses of big sagebrush (*Artemisia tridentata*) to abiotic conditions. *Ecological Modelling*
711 286:66–77.

712 Schlaepfer, D., W. K. Lauenroth, and J. B. Bradford. 2014b. Natural Regeneration Pro-
713 cesses in Big Sagebrush (*Artemisia tridentata*). *Rangeland Ecology & Management* 67:344–
714 357.

715 Schlaepfer, D., W. K. Lauenroth, and J. B. Bradford. 2012. Effects of ecohydrological
716 variables on current and future ranges, local suitability patterns, and model accuracy in
717 big sagebrush. *Ecography* 5:453–466.

718 Schurr, F. M., J. Pagel, J. S. Cabral, J. Groeneveld, O. Bykova, R. B. O’Hara, F. Har-
719 tig, W. D. Kissling, H. P. Linder, G. F. Midgley, B. Schröder, A. Singer, and N. E. Zim-
720 mermann. 2012. How to understand species’ niches and range dynamics: A demographic
721 research agenda for biogeography. *Journal of Biogeography* 39:2146–2162.

722 Shafer, S. L., P. J. Bartlein, and R. S. Thompson. 2001. Potential changes in the distri-
723 butions of western North America tree and shrub taxa under future climate scenarios.
724 *Ecosystems* 4:200–215.

725 Shriver, R. K. 2015. Quantifying how short-term environmental variation leads to long-
726 term demographic responses to climate change. *Journal of Ecology*:n/a–n/a.

727 Stan Development Team. 2014a. Stan: A C++ Library for Probability and Sampling,
728 Version 2.5.0.

729 Stan Development Team. 2014b. Rstan: the R interface to Stan, Version 2.5.0.

730 Still, S., and B. Richardson. 2015. Projections of Contemporary and Future Climate Niche
731 for Wyoming Big Sagebrush (*Artemisia tridentata* subsp. *wyomingensis*): A Guide for

- 732 Restoration. *Natural Areas Journal* 35:30–43.
- 733 Vanderwel, M. C., V. S. Lyutsarev, and D. W. Purves. 2013. Climate-related variation in
734 mortality and recruitment determine regional forest-type distributions. *Global Ecology*
735 and *Biogeography* 22:1192–1203.
- 736 Wikle, C. K. 2010. Low-rank representations for spatial processes. Pages 89–106 *in* A.
737 Gelfand, P. Diggle, M. Fuentes, and P. Guttorp, editors. *Handbook of spatial statistics*.
738 Chapman; Hill, Upper Saddle River, New Jersey, USA.
- 739 Xian, G., C. G. Homer, and C. L. Aldridge. 2012. Effects of Land Cover and Regional
740 Climate Variations on Long-Term Spatiotemporal Changes in Sagebrush Ecosystems. *GI-*
741 *Science & Remote Sensing* 49:378–396.